Chemical Physics 143 (1990) 305–323
North-Holland

STATE-SELECTIVE IONIZATION OF NITROGEN BY RESONANCE-ENHANCED THREE- AND FOUR-PHOTON EXCITATION

S. OPITZ [1], D. PROCH, T. TRICKL [2] and K.L. KOMPA
Max-Planck-Institut für Quantenoptik, D 8046 Garching, FRG

Received 2 November 1989

Several efficient approaches for the generation of vibrationally cold nitrogen ions by resonance-enhanced multi-photon ionization are examined. More than 10^5 ions per laser pulse are demonstrated for single-laser, 2+1 photon ionization via a $^1\Pi_g(v'=10)$ which accesses only the $v_+=0$ level of the ion. The rotational distribution of the photoions is analysed by laser-induced fluorescence under molecular beam conditions. A $\Delta N=0$ rotational propensity rule is found for the ionizing step when ionizing out of the Π^+ component of the a $^1\Pi_g$ state. In addition, two-laser 2+1+1 photon ionization with a $^1\Pi_g$ and $c_4' \, ^1\Sigma_u^+$ or $c_3 \, ^1\Pi_u$ vibrational levels as the intermediates is investigated. With the excitation of $a(v'=4)$ and c_4', $c_3(v=0)$ strong ion signal is detected for an excess energy above the ionization threshold of about 16400 cm^{-1}, which yields $X \, ^2\Sigma_g^+$ $(v_+=0)$ as well as $A \, ^2\Pi_u$ ions, but no signal at about 7500 cm^{-1} which would confine the ionic state distribution to $X \, ^2\Sigma_g^+$ $(v_+=0)$. Ionization via $a(v'=1)$ and $c_3(v=0)$ is investigated as an alternative scheme to produce $v_+=0$ ions. Though not being as efficient as the 2+1+1 photon ionization involving some of the $c_n'(v)$ states this excitation scheme yields 5×10^4 ions per laser pulse. A first experiment to prepare N_2^+ in the $v_+=1$ level is carried out.

1. Introduction

One of the most crucial conditions for investigations of reactive collisions of molecular ions is the knowledge of their initial state. The complex electronic structure and large cross sections of ionic processes suggest careful control of the experimental parameters. Several concepts have been used for state discrimination. Considerable success has been obtained by the photoion–photoelectron coincidence technique by which one can trace the influence of different vibrational levels of the reactant ions in ion–molecule reactions [1–4]. In addition to this, great effort is spent on the development of sources of state-selected ions. The advantages of such sources are that the entire ion current becomes available for the experiment rather than a small fraction selected from a large manifold of occupied states in the beam, and that some more refined state selection is possible.

Internally cold ions can be prepared by adiabatic cooling in a molecular beam. Johnson et al. [5] studied laser-induced fluorescence (LIF) of CO^+ generated by electron bombardment and subsequent cooling in a jet expansion. They found that 99% of the population was in the $v_+=0$ level with a rotational temperature of 10–20 K. This method is restricted to light molecules for which no vibrational cooling is necessary. Complete rotational cooling may also be hard to achieve.

All other experiments with state-selected ions use photoionization techniques for their generation which are more versatile. This includes lower rotational excitation as well as controlled preparation of molecular ions in single vibrational levels with no restriction to just $v_+=0$.

The classical example is the single-photon ionization of H_2 studied under high resolution by Chupka et al. [6,7]. The ionization of H_2 near threshold is dominated by autoionization of Rydberg states which proceeds with minimum change of the vibrational quantum number. H_2^+ vibrationally selected in this

[1] Present address: MBB-Medizintechnik G.m.b.H., Postfach 801168, D 8000 Munich 80, FRG.

[2] Present address: Fraunhofer-Institut für atmosphärische Umweltforschung, Kreuzeckbahnstrasse 19, D 8100 Garmisch-Partenkirchen, FRG.

manner has been collided with various atoms and molecules [8–12].

With the advent of powerful pulsed lasers and efficient frequency-doubling, resonance-enhanced multi-photon ionization (REMPI) has become attractive. State selection of the ions is achieved by suitable choice of the intermediate resonance(s). REMPI with short laser pulses also opens the important option of high-resolution time-of-flight energy and mass analysis.

The most preferable state-selective excitation schemes are those for which the final intermediate level is part of a Rydberg state. Such states possess perfect Franck–Condon overlap with the ionic potential curve. Thus, the vibration does not change during the ionization.

A general propensity rule for vibrational state selection in photoionization out of an excited state was suggested by Meek et al. [13,14] after studies of toluene and benzene. The state-selectivity of 2+1 and 3+1 photon ionization with transition to a Rydberg state as the first step was demonstrated by photelectron spectroscopy (PES) for the formation of NO^+, H_2^+, N_2^+ (A) and NH_3^+ [15–21]. Conaway et al. [22,23] subsequently studied the state-specificity of the reactions of NH_3^+ (v) with D_2 and CH_4.

Photoionization methods also offer the potential for perfect or nearly perfect rotational state selection. Rotational angular momentum transfer in photoionization is restricted to just a few quanta, depending on the number of partial waves of the outgoing electron. This fact, together with the validity of selection rules for $n+1$ photon ionization [24], has been shown in a number of experiments with high-resolution PES [25–34] and LIF [35].

It has been the goal of our work to demonstrate the suitability of REMPI for the generation of intense state-selected pulsed ion beams for molecules with rather high ionization energies. As a first example we have studied the three- and four-photon ionization of N_2 for which abundant spectroscopic data on high-lying states are available [36]. A preliminary account of our results was given previously [#1].

N_2 is a REMPI suitable molecule (see fig. 1). Many of the excited states and the ionic ground state exhibit favourable Franck–Condon overlap with the $X\,^1\Sigma_g^+$ state of the neutral molecule. Several Rydberg series are known and analysed in great detail. Experimental problems for the generation of an intense, state-selected N_2^+ beam arise from the fact that the lowest-lying singlet state which may serve as a first intermediate is located as high as 8.4 eV. Another disadvantage is the strong interaction of many Rydberg states belonging to series which converge to the ground state of N_2^+ with neighbouring electronic states [36]. Pratt et al. [38] have shown by photoelectron spectroscopy in a 3+1 photon ionization experiment via the c_3 and c_4' Rydberg states that ionization out of such a perturbed state with high excess

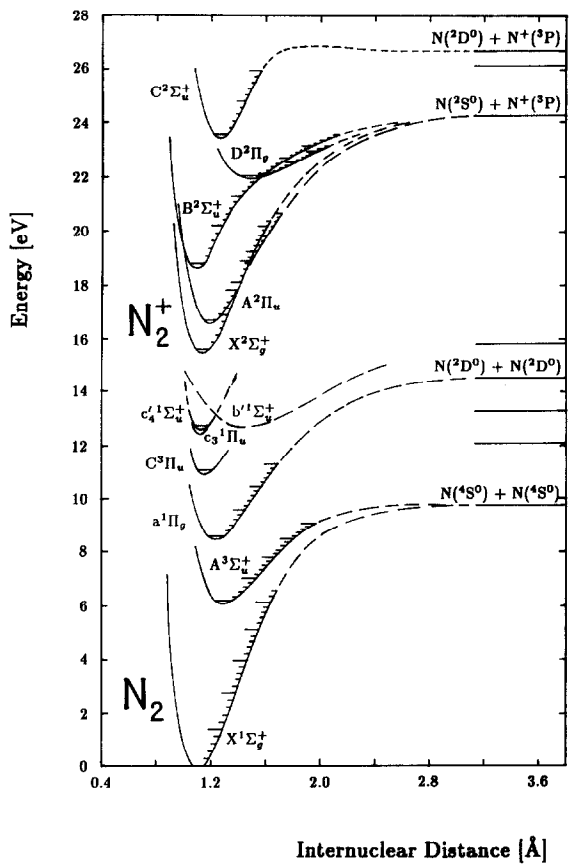

Fig. 1. Potential energy diagram of N_2 with the states which are most important for this study (the potential energy curves were taken from ref. [36]).

[#1] A selection of our results has been presented at the 1986 CLEO conference [37].

energy does not necessarily yield a single electronic state of the ion. Due to the mixing of the c_3 and c'_4 states with states which allow the generation of $N_2^+(A)$ in a single-electron transition, in most cases a substantial fraction of the N_2^+ ions is created in the $A\,^2\Pi_u$ state.

All our experiments involve the $a\,^1\Pi_g$ state of N_2 as the first intermediate state, excited by two photons from a frequency-doubled dye laser. The next step is ionization with one or two additional photons from the same or a second laser. In the case of a two-colour experiment the second laser is tuned to transitions from a $^1\Pi_g$ to the c_3 and c'_4 Rydberg states of N_2. The two-laser excitation scheme infers some flexibility over the rigid 3+1 photon ionization scheme of ref. [38] because the frequency of the second laser can be varied in discrete steps by exciting different vibrational levels in the a state with the first laser. For sufficiently high v' the excess energy of the ionizing step (pumped by laser 2) can be reduced to values below the A state threshold. The unwanted A state contributions observed in the photoelectron spectra [38] can, thus, be avoided. Also, the use of two resonances instead of one results in an enhanced ion yield for given laser intensities.

The $B \rightarrow X$ transition of N_2^+ has a fluorescence lifetime of 61.35(30) ns [39]. This facilitates an analysis of the photoions by LIF. The Franck–Condon factors are favourable: 0.65 for the (0, 0) band and 0.30 for the (1, 0) band [36]. Application of the LIF method to the ion beam requires more than 10^4 ions per pulse, provided that only a few rotational states are populated. The low efficiency is due to losses in fluorescence collection and detector sensitivity.

The LIF technique, in spite of its limited sensitivity, has one important advantage over ultra-high resolution PES as described in refs. [30,31,33,34]. It can be used for the rotational analysis of dense ion bunches as generated in REMPI sources. Effects of the ionic long-range interactions, which may become important with the onset of space-charge formation, can therefore be monitored.

The following experiments are discussed in this paper:

(1) Preparation of $N_2^+\ X\,^2\Sigma_g^+\ (v_+ = 0)$ by single-colour, 2+1 REMPI via a $^1\Pi_g(v' = 10)$.

(2) Rotational analysis of the ions created by experiment (1) by LIF.

(3) Two-colour experiments with $c'_4\ ^1\Sigma_u^+$ and $c_3\ ^1\Pi_u$ ($v = 0, 1$) as the final intermediate states.

In addition, we obtained detailed spectroscopic results on the $a \leftarrow X$ transition of N_2 by 2+2 REMPI and on non-Franck–Condon behaviour of this REMPI process which will be published separately [40].

2. Experimental

A schematic view of our ion-beam experiment is shown in fig. 2. The apparatus consists of four differentially pumped sections: the ion source, a drift region with ion optics, a 90° magnetic mass separator and the main chamber containing a second set of ion optics (identical to that in the drift region) and a microchannel-plate ion detector. In the future, the main chamber will be equipped with a scattering gas cell and a mass spectrometer for reactive scattering experiments. The ion beam path between source and detector is roughly 1 m long.

The ions are prepared in the intersection between the laser beam and a synchronously pulsed molecular beam. These two beams and the direction of ion extraction are mutually perpendicular. The photo-excitation occurs inside a commercial crossed-beam ion source (Balzers) which was modified to allow unobstructed passage of both beams. This unit contains a small electron gun for electron-impact ionization of the jet. This permits quick performance checks of the components along the ion beam.

The elements of the molecular beam source are a piezoelectric valve of local design, with a nozzle diameter of 0.20 mm, and a skimmer (Beam Dynamics, model 1, orifice diameter 1.0 mm, mounted on a teflon cap) for collimation of the jet. The distance between nozzle and laser focus is 45 mm. We use a piezoelectric valve because of the absence of magnetic fields and because of the low level of rf noise. Our new design overcomes most of the shortcomings of previous models. In particular, it is capable of producing unchoked gas flow for large nozzles (diameter up to 1.0 mm) and can be operated with high backing pressures. A description is given in a separate publication [41].

The ions are accelerated to approximately 0.9 keV and collimated by the extraction optics. Further con-

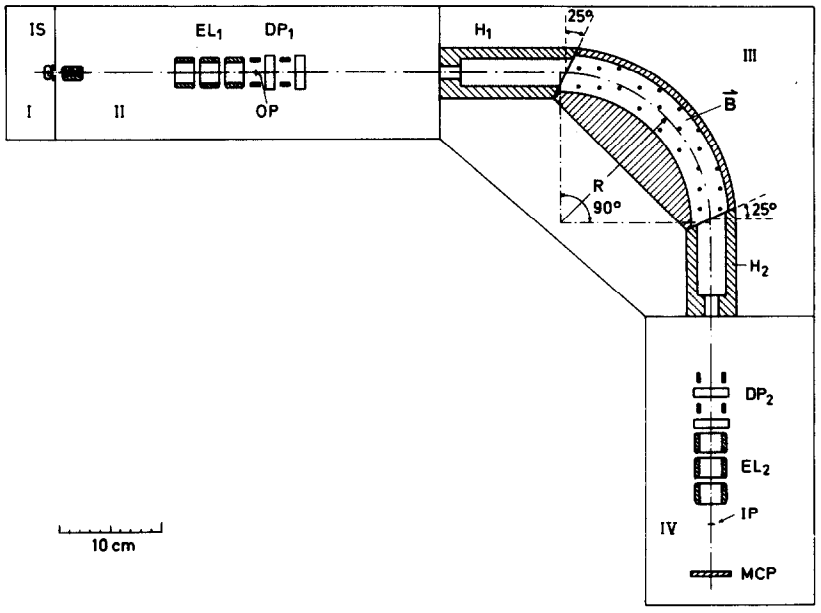

Fig. 2. Schematic diagram of the ion-beam apparatus: I ion source chamber, II beam adjustment region, III mass separator, IV main chamber, IS ion source, EL electrostatic lens, DP deflection plates, H Herzog aperture, OP object plane of mass separator, IP image plane of mass separator, MCP microchannel plate.

trol of the ion beam is achieved by the ion optics in section II and at the main chamber entrance. Both sets of ion optics consist of an "einzel" lens and four pairs of deflection plates which allow parallel displacements of the beam. Activation of these plates was usually unnecessary.

The 90° mass separator consists of a 40° magnet terminated by two 12 mm wide Herzog apertures at their respective ends. The beam radius is 150 mm. Both apertures are made of gold-plated iron which provides a rather defined boundary for the magnetic field. The faces of the apertures which contact the magnet intersect the ion beam at an angle of 25° (see fig. 2). Thus, horizontal as well as vertical focusing of the ion beam is achieved [42]. The mass separator is set up for maximum transmission rather than for perfect mass resolution. However, $m/\Delta m$ values of more than 50 were observed for N_2^+ with moderate ion currents. For high currents corresponding to more than 5×10^3 ions per pulse the mass resolution was reduced, mainly because of the onset of detector saturation of the double-microchannel-plate ion detector (Galileo, CEMA 3025).

All sections of the apparatus, except the ion source, are evacuated to less than 10^{-7} mbar by turbomolecular pumps. The ion source is equipped with a combination of a turbomolecular pump and a 14 K cryo panel which maintain the average pressure at about 1×10^{-6} mbar with the valve operating at 10 Hz and ensure a hydrocarbon-free environment for the photoexcitation volume.

For the LIF experiments the molecular beam source was transferred to a separate chamber with light baffles to minimize scattered laser light and with a fluorescence detection system. This detection system consists of four lenses, an aperture for spatial filtering and a photomultiplier tube (VALVO, XP2020, maximum sensitivity at 400 nm), and has an effective acceptance cone angle of 40°. The focus of the ionizing laser was located 5 mm away from the nozzle where the beam was nearly completely cooled as verified by REMPI. Setting the detection gate width to 150 ns additionally helped to ensure collision-free conditions. The LIF laser was unfocused.

The generation and analysis of the ions required three excimer-laser pumped dye lasers (all Lambda

Physik, FL2002 with FL582 computer control). The two REMPI lasers (laser 1, laser 2) shared the same pump laser (Lambda Physik, EMG200), whereas the LIF laser (laser 3) was pumped by a separate unit (Lambda Physik, EMG100). The laser which excited the a←X two-photon transition of N_2 (laser 1) was equipped with an intracavity etalon which reduced the bandwidth from 0.2 to 0.03 cm^{-1}. Laser 1 was then frequency doubled with KDP or BBO crystals with up to 20% energy conversion efficiency resulting in up to 4 mJ of UV pulse energy. Typical repetition rates were 3–10 Hz, the upper limit being determined by the pump laser. For laser beam steering we used dielectric mirrors and beam combiners in order to minimize losses. The laser pulse energies, as cited in the following, were measured after passage through the ion source chamber and a rotatable Brewster exit window with a pyroelectric detector (Laser Precision, Rpj 7200).

The REMPI signal which exhibited typical shot-to-shot fluctuations of 30% was fed into a boxcar integrator (Stanford Research Systems) and integrated over 10–30 shots. In the LIF experiments, the output of the photomultiplier tube was registered by a gated photon counter (Stanford Research Systems, model SR400).

The control of the entire experiment and the data acquisition was managed by a PDP11 microcomputer which was connected to the various components by a CAMAC system. Data were collected from the boxcar integrator (REMPI), the photon counter (LIF), and the laser energy meters.

3. Results

3.1. Survey of the experiments

Typical conditions for the REMPI and LIF experiments of this study are listed in table 1. The excitation schemes for the three experiments which are specified in table 1 are visualized in fig. 3.

3.2. Signal optimization

In view of future ion-beam scattering experiments it has been one of our main goals to determine the upper limit for the ion-beam current which can be generated under the present experimental conditions. The essential parameters for the optimization are the laser pulse energy and the gas pressure in the molecular beam source. For both, however, there are limitations. The ultraviolet (UV) pulse energy does not exceed a few millijoules for our excimer-laser-based system, particularly in the case of two-laser ionization when the pump laser beam is split between both dye lasers. Increasing the N_2^+ signal by enhancement of the backing pressure P_0 in the pulsed valve was successful only up to 4.0 bar. Above 4.0 bar there was additional improvement by not more than

Table 1
Experimental conditions

	2+1 REMPI via a($v'=10$) (with LIF experiment)	2+1+1 REMPI via a($v'=4$) and c, c' ($v=0$)	2+1+1 REMPI via a($v'=1$) and c, c' ($v=0$)
laser dye (laser 1)	coumarin 102	coumarin 153	coumarin 153
laser dye (laser 2)	–	PTP	rhodamine 6G
laser dye (laser 3)	QUI	–	–
pump energy ratio for laser 1 and laser 2	–	50:50	70:30
pulse energies [a] (mJ) (laser 1)	0.03–1.0 (2ω, BBO)	0.1–3.8 (2ω, KDP)	0.1–2.7 (2ω, KDP)
pulse energies [a] (mJ) (laser 2)	–	0.0005–5.5 (ω)	0.001–0.5 (2ω, KDP)
pulse energies [a] (mJ) (laser 3)	0.1–1.0	–	–
focal lengths (cm) (laser 1)	7.5, 10, 20	20, 35	20, 35

[a] Measured at the ion source.

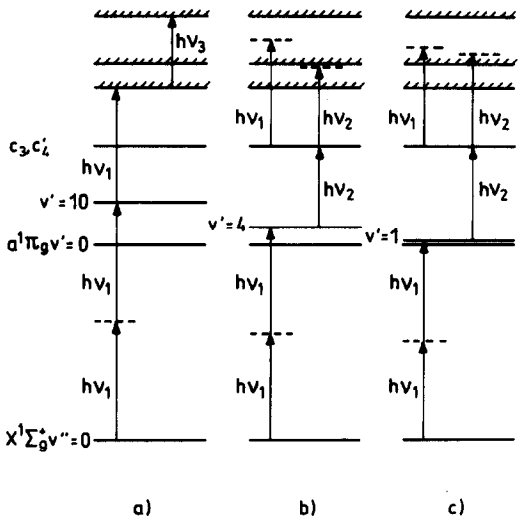

Fig. 3. Diagrams of the most important excitation schemes used in this work. (a) 2+1 single-colour ionization via a($v'=10$) followed by LIF diagnosis of the photoions. (b) 2+1+1 REMPI with two lasers via a($v'=4$) and $c_3(v=0)$ or $c_4'(v=0)$. (c) 2+1+1 REMPI with two lasers via a($v'=1$) and $c_3(v=0)$ or $c_4'(v=0)$.

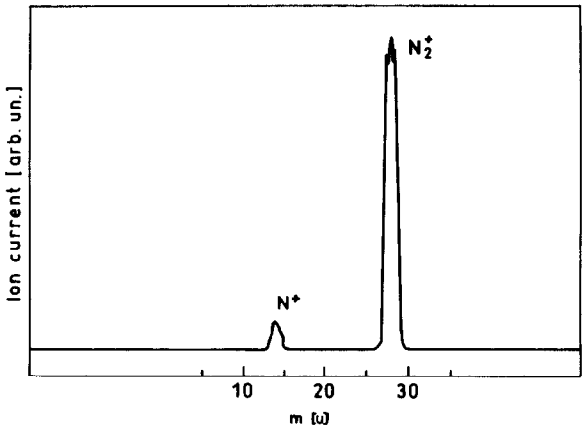

Fig. 4. Mass spectrum of nitrogen ionized by 2+2 REMPI with the (3, 0) S_0 line of the a←X transition excited in the first step; 1.2 mJ UV were focused into the ion source with an $f=7.5$ cm lens. The atomic contributions result from the strong focusing of the UV beam. The wavelength spectra for N^+ and N_2^+ are indistinguishable which establishes a $^1\Pi_g$ as common precursor. The substantial broadening of the mass peaks is mainly due to detector saturation (we estimate nearly 10^6 ions per laser pulse).

10%. This levelling-off, which was also present with the skimmer removed, was examined with low laser power to exclude detector saturation. It can, thus, be ascribed to gas reflected into the beam from nearby walls. For elevated pressures, the gas pulse length was drastically reduced due to this effect as determined by measuring the population of the $J''=0$ rotational level as a function of the laser decay. The experiments were usually run with $P_0=3.0$ bar.

Another limitation results from the onset of Coulomb repulsion of the ions formed in the small laser focus. This space-charge effect is responsible for transverse velocity components which may cause ion losses at the apertures along the 1 m flight path. These transverse components may already exceed 1% of the forward ion-beam velocity if one generates more than 10^4 ions in a focus of less than 0.1 mm diameter, as we estimate from a simplified solution of the equations of motion. We observed considerable stretching of the ion bunches by roughly a factor of five (from 60 to about 300 ns) as the production rate approached 10^5 ions per pulse. However, because of the onset of detector saturation in the same signal regime we can only partly attribute this observation to space-charge effects.

Strong focusing causes some additional problems. Fig. 4 shows a mass spectrum obtained by scanning the magnetic field of our mass spectrometer. N_2^+ is generated by single-colour, 2+2 photon ionization via a $^1\Pi_g(v'=3)$ with 1.2 mJ UV from laser 1 focused by an $f=7.5$ cm lens. Apart from the N_2^+ peak we observe a second, smaller signal due to atomic nitrogen. The formation of N^+ ions requires the absorption of at least two additional photons because of the high dissociation energy of N_2^+ of 8.71 eV [36]. The N^+ peak shows exactly the same a←X spectral dependence as the N_2^+ peak which establishes the a $^1\Pi_g$ state as common precursor.

The occurrence of six-photon dissociative ionization shows that it is easily possible to prepare undesired electronically excited ions. Their appearance can be minimized by reducing the intensity by the choice of proper focusing conditions. Most of our experiments were therefore carried out with larger focal lengths. With an $f=20$ cm lens, e.g., no N^+ ions were observable for the strong 2+2 REMPI via a($1\leqslant v'\leqslant 4$) (favoured by the largest Franck-Condon factors of the (v', 0) band progression [36]) for

more than 2 mJ of incident pulse energy. The N_2^+ signal thresholds were between 50 and 100 μJ for the strongest rotational line (S_0).

In a loss-free n photon process the number N_e of excited molecules (or photoions) is approximately expressed by

$$N_e \approx N \times I^n \approx f^4/f^{2n}, \quad (1)$$

with N being the number of molecules in the laser focus and I the intensity of the UV beam [43]. Hence, the population in the two-photon excited a $^1\Pi_g$ state does not depend on the focal length ($n=2$) as long as the effective length of the focus does not exceed the gas beam diameter. E.g., in the case of the two-colour ionization scheme

$$N_2^+ \leftarrow c_4' \leftarrow a \leftarrow N_2(X),$$

the ion signal did not decrease significantly when we replace the initially used $f=20$ cm lens by an $f=35$ cm lens which indicates saturation of the two transitions between the a state and the continuum and which proves the independence of the a state population of f. However, the 2+2-photon-induced background due to single-colour excitation with laser 1 is substantially reduced by the choice of the $f=35$ cm lens because this signal scales nearly as f^{-4} (see eq. (1)).

Under these low-intensity conditions the a←X lines are very narrow due to the absence of the ac Stark effect which is observed with shorter focal lengths [40]. For improved matching of laser bandwidth and absorption width we operated laser 1 with an intracavity etalon. The observed UV linewidths were 0.05 cm^{-1}.

3.3. Generation of cold N_2^+ ions by single-colour 2+1 REMPI

Vibrationally cold N_2^+ can be produced in a rather simple way with just one frequency-doubled dye laser tuned to a wavelength of 237 nm. a $^1\Pi_g(v'=10)$ serves as intermediate level. This choice allows ionization by a third 237 nm photon with an excess energy of just 903.3 cm^{-1} (S_0 line) [40,44]. The $v_+=1$ level of N_2^+ lies 2174.75 cm^{-1} above the ionization threshold [45]. Therefore, population of vibrational levels of the $X\,^2\Sigma_g^+$ state with $v^+ \geq 1$ as well as population of higher electronic states of N_2^+ is avoided,

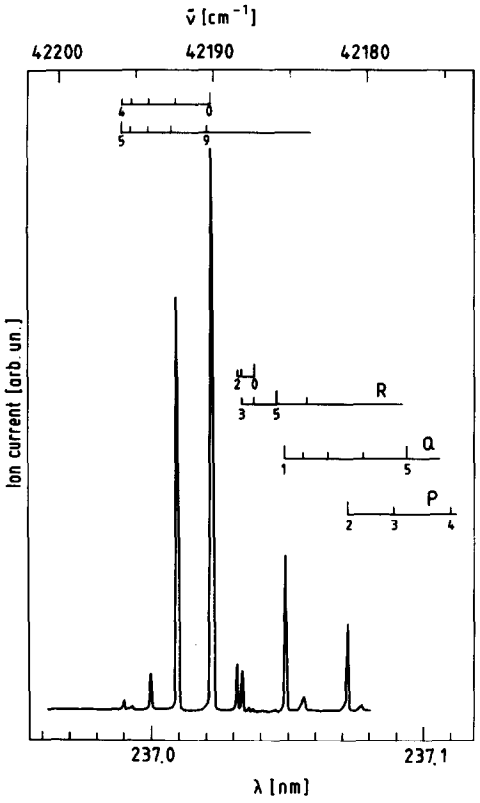

Fig. 5. 2+1 REMPI spectrum of N_2; laser 1 is tuned across the a←X (10, 0) transition. The strongest lines are reduced in size and broadened due to the onset of detector saturation.

provided that one excludes 2+2 photon ionization by a proper choice of the focal length as described above.

Fig. 5 shows a scan of laser 1 across the (v', v'') = (10, 0) band. The parameters are 0.5 mJ UV energy and $f=20$ cm. The strongest lines are those of the S branch. Only three rotational levels of N_2 are populated ($J'' \leq 2$) in the molecular beam corresponding to a rotational temperature of 8 ± 1 K. For the S_0 line nearly 10^5 ions per pulse were detected by the microchannel plate. This is quite remarkable if one considers the small Franck–Condon factor of the (10, 0) band which is just about 1/20 of that of the strongest (v', 0) band ($v'=3$). It is explained by saturation of the ionizing step which is a single-photon transition in this case, whereas for lower intermediate v' the ionizing step is a less efficient two-photon

transition. This argument is supported by the observation of a nearly quadratic dependence of the ion signal on the laser pulse energy in the region below the onset of ion detector saturation.

The levels of the a $^1\Pi_g$ state with $v' \geqslant 6$ are known to predissociate [#2]. The linewidth for the (10, 0) band does not exceed the excitation bandwidth by more than 0.010 cm^{-1} which means a lifetime of more than 0.27 ns. This proves that this predissociation is rather slow as one could already conclude from the observation of emission for high gas pressures by Herman [#3].

3.4. Laser-induced fluorescence of the $v_+ = 0$ photoions

The ions generated by the 2+1 photon ionization scheme described in section 3.3 were rotationally analysed by exciting the B←X (0, 0) band of N_2^+ with laser 3. In order to inhibit any influence of laser 3 on the photoionization process this laser was delayed by 30 ns with respect to laser 1. The fluorescence detection gate was opened another 30 ns later. By this timing, the residual scattered light which was not captured by the baffle system could be suppressed almost quantitatively. However, delayed detection causes a loss of fluorescence signal due to the short lifetime of the N_2^+ B→X transition of 61.35(30) ns [39]. The gate width was 150 ns. The pulse energies of lasers 1 and 3 were, both, 1 mJ.

Figs. 6a and 6b show the LIF spectra for ionization via the a←X S_0 and S_1 transitions, respectively. The spectra each exhibit a P and an R branch and reveal population in just three ionic rotational levels, those with $N_+ = J'$ and $N_+ = J' \pm 1$ (J' being the a-state rotational quantum number). The population in the $N_+ = J'$ level exceeds that in the neighbouring ones by roughly a factor of three. The pulse energy of laser 3 was adjusted to saturate the transition with the unfocused beam for optimum sensitivity. The saturation broadening results in a linewidth of about 0.75 cm^{-1} in both spectra.

[#2] The $v' = 6$ level predissociates above $J' = 13$, see ref. [36].
[#3] See refs. [36,46,47].

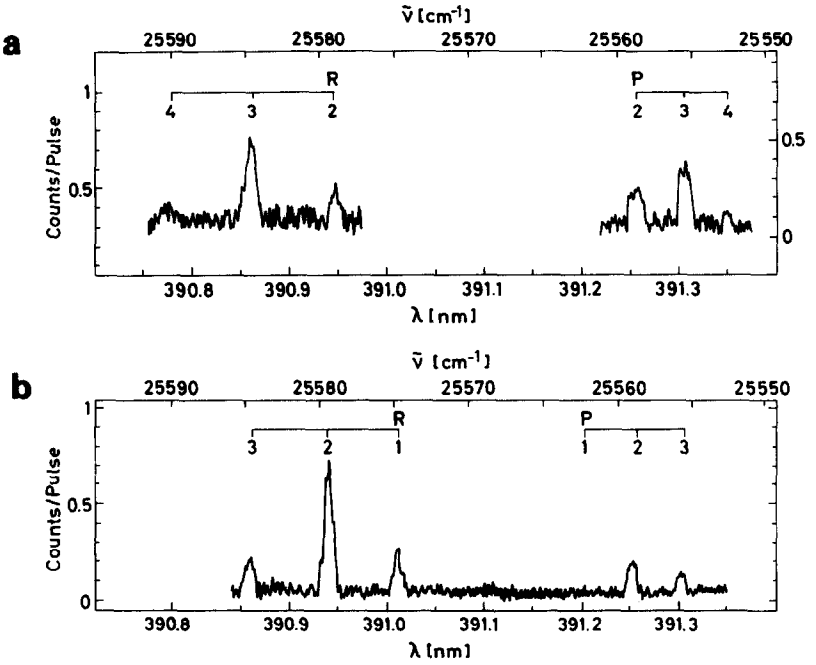

Fig. 6. Laser-induced fluorescence of the N_2^+ photoions which are generated by 2+1 REMPI with laser 1; the B←X (0, 0) band of N_2^+ is excited by laser 3. Laser 1 is tuned to the a←X (10, 0) transition. (a): S_0, (b): S_1.

A different rotational selection rule for ionization may be expected for the excitation of the a←X P and R branches, as will be discussed in more detail in section 4. However, because of the much lower ion yield compared with S branch excitation attempts to measure LIF for R or P lines (see fig. 5) have not been successful.

The low level of the LIF signal, also, prevented the determination of the relative population of excited vibrational levels which might originate from 2+2 photon ionization. Furthermore, no easy way is seen to measure the A state population due to such a 2+2 photon process. As to the excited states of N_2^+, $B\,^2\Sigma_u^+$, $C\,^2\Sigma_u^+$ are not accessible in a single-photon transition and the $D\,^2\Pi_g$ state is shifted to longer internuclear distances which implies a bad Franck–Condon overlap with the A state. The Franck–Condon factor for the D→A (0, 0) band is 2.6×10^{-6} [48].

There are, however, several experimental hints which indicate the existence of 2+2 photon effects for the conditions of this LIF experiment:

Firstly, there are the results of the two-colour experiments via $a(v' \leqslant 4)$ (see sections 3.2 and 3.5) which suggest softer focusing of laser 1 for elimination of this additional ionization channel.

Secondly, in an earlier experiment with $f=7.5$ cm, we observed ion signals when tuning laser 1 to the a←X (8, 0) and (9, 0) bands. In this case, for energetic reasons, ionization cannot be due to a 2+1 process. At least four photons are required for ionization. For about the same UV intensity of laser 1 in the focus as used for the N_2^+ generation in the LIF experiment ($f=20$ cm) we observed approximately 20 and 60% of the (10, 0) ion signal for (8, 0) and (9, 0), respectively. The Franck–Condon factors for the (8, 0), (9, 0) and (10, 0) bands are 0.0315, 0.0178 and 0.0098 [36]. This would suggest smaller 2+2 photon contributions for the (10, 0) pathway than for the (8, 0) and (9, 0) routes, provided that there is no local enhancement of the ion yield due to energy levels near the three- or four-photon energy. Such a "resonance" is obviously observed for the (9, 0) case, as one can see from a comparison of the above relative ionization rates with the Franck–Condon factors. Astonishingly, we found anomalously high dissociative ionization when exciting the (9, 0) band: about three times more N^+ than N_2^+ ions were recorded in the experiment with the $f=7.5$ cm lens.

The third indication of 2+2 photon ionization can possibly be derived from the LIF spectra (fig. 6). The coexistence of rotational levels of both parities should not be possible for single 2+1 photon ionization of the homonuclear molecule N_2. Nevertheless, we observe some population in ionic rotational levels with $N_+ = J' \pm 1$ in addition to the prevailing population in the $N_+ = J'$ level (see also section 4.1).

3.5. Generation of cold N_2^+ ions by two-colour REMPI

The 2+1 photon ionization of N_2 near threshold as described in the previous sections provides a rather simple way for the generation of vibrationally cold N_2^+ if one controls the focusing conditions properly. The use of two tunable lasers offers the possibility to excite the c_n, c'_m Rydberg states as the final intermediate states. Because of the excellent Franck–Condon overlap of these Rydberg states with the ionic ground state [38] X state ions should be formed in the same vibrational level as was prepared in the Rydberg state. This opens another way for producing cold N_2^+, but also a way for defined vibrational excitation of the ions (see section 3.6). Due to the additional resonance, copious ions may be created without pumping the a←X two-photon transition too hard. Pratt et al. [38] showed by PES that, indeed, reasonably good vibrational state selectivity of N_2^+ $X\,^2\Sigma_g^+$ may be obtained in this way for $c_3\,^1\Pi_u(v=0, 1)$ and $c'_4\,^1\Sigma_u^+(v=0, 1)$ as the final intermediate levels. Their excess energies, however, determined by their single-colour 3+1 photon ionization scheme, range between as much as 13400 cm^{-1} and 16200 cm^{-1}, well above the $A\,^2\Pi_u$ state threshold (9016.021(8) cm^{-1} [49]). With one exception ($c_3(v=0)$), A state contributions are observed in the photoelectron spectra which are of similar magnitude as the X state signal.

Formation of electronically excited N_2^+ may be avoided by keeping the frequency of the ionizing dye laser sufficiently low. In a two-colour experiment, this is achieved by exciting a $^1\Pi_u(v' \geqslant 4)$ as the first intermediate level. With laser 2 tuned to the transitions from this level to $c'_4(v=0)$ or $c_3(v=0)$ and ionization with laser 2 the excess energy becomes less than about 7500 cm^{-1}, which is well below the A state onset. Ionization with UV from laser 1, which would

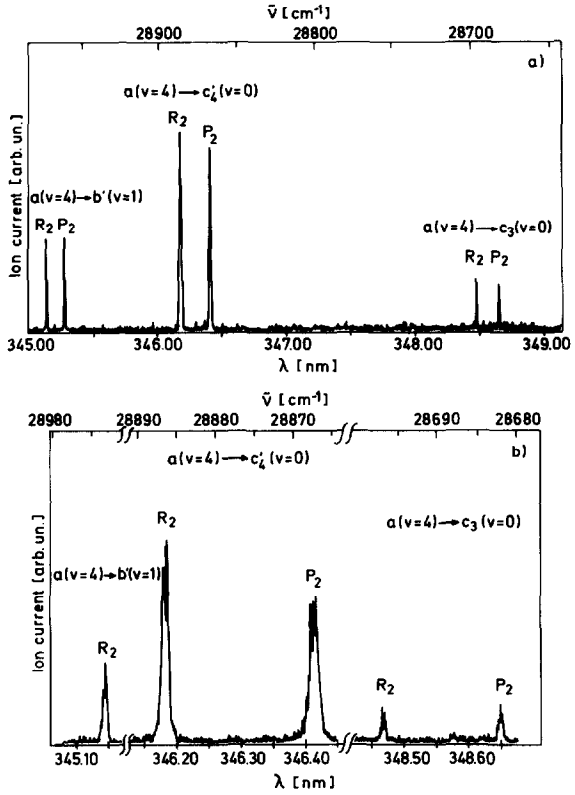

Fig. 7. Scans of laser 2 across the transitions from the a $^1\Pi_g(v'=4, J'=2)$ level to the $c'_4(v=0)$ and $c_3(v=0)$ Rydberg states as well as to the b' $(v=1)$ state; strong enhancement of the ion signal is observed if laser 2 hits a resonance (see text). The lower trace (b) depicts expanded partial scans of the P–R doublets. The zero signal level is shifted up in both traces for convenience and corresponds to the minimum signal positions.

result in an excess energy of 16381 cm^{-1}, can be excluded by delaying laser 2.

Fig. 7a shows a scan of laser 2 across the region of the $c_3 \leftarrow a$ (0, 4) and $c_4 \leftarrow a$ (0, 4) bands with laser 1 set to the S_0 line of the $a \leftarrow X$ (4, 0) band. The conditions of this scan were 1.7 mJ of UV from laser 1, 60 μJ from laser 2, $f=35$ cm (both beams collinear, f being longer by about 5 mm for laser 2 due to the chromatic aberration) and no delay between the pulses of the two lasers. The polarizations of the two lasers were parallel. The 2+2 photon background is nearly 1/100 of the maximum signal and corresponds to the baseline noise. Three line doublets are seen which represent the R_2 and P_2 lines of the b' $\leftarrow$a (1, 4), $c'_4 \leftarrow$a (0, 4) and $c_3 \leftarrow$a (0, 4) bands. The Q_2 line of the $c_3 \leftarrow$a transition should be observable ($^1\Pi_u \leftarrow {}^1\Pi_g$), but is missing. It appears for pulse energies near 1 mJ. The 2+2 photon background due to laser 1 is less than 1% of the resonant signal (see section 3.2).

Under our conditions, the three bands of fig. 7 are saturated by laser 2 with more than 300, 0.5 and 15 μJ, respectively. As can be seen from fig. 7b, which shows scans of laser 2 across the doublets in fig. 7a with expanded frequency scale, the lines are strongly broadened, particularly those of the $c'_4 \leftarrow$a band which have the lowest saturation threshold. Below the saturation thresholds the linewidth was about three times the specified bandwidth of laser 2 which possibly indicates some additional influence of the intense laser 1. The ionizing step is saturated out of $c'_4(v=0)$ and b' $(v=1)$ but not out of $c_3(v=0)$.

The influence of the polarizations of the two lasers on the two-colour REMPI signal was examined by placing a UV Fresnel rhomb (Halle) in one of the two beams. A few tests were carried out within the $c'_4 \leftarrow$a and $c_3 \leftarrow$a (0, 4) bands which did not reveal any evidence of polarization effects.

Subsequently, we delayed laser 2 by 15 ns with respect to laser 1 by using a 5 m optical delay line. The spectrum, still, showed roughly the same b' $\leftarrow$a and $c'_4 \leftarrow$a line intensities, though there is very little temporal overlap of the two laser pulses. The $c_3 \leftarrow$a lines were smaller by nearly one order of magnitude. This indicates that for the $c_3 \leftarrow$a pathway ionization is mainly achieved by a third UV photon from laser 1.

The long lifetime of the stable levels of the a $^1\Pi_g$ state (56.2 μs for, e.g., $v' \leqslant 2$ [50]) allows complete temporal separation of the two laser pulses. Ionization out of one of the two Rydberg states or the b' $(v=1)$ state is then only possible with laser 2. However, after extending the delay to 30 ns no two-colour-induced signal could be detected at all. Even for more than 5 mJ from laser 2 in the ion source, corresponding to nearly 5 GW/cm^2, merely the 2+2 photon background was seen with laser 2 tuned to any of the c'_4 lines (an $f=20$ cm lens was used is this case).

The absence of a two-colour ion signal for ionization with laser 2 is quite surprising since the results for 15 ns delay show that rather low intensity of laser 1 is required for saturated (or near-saturated) ionization out of the $c'_4(v=0)$ level for this higher excess

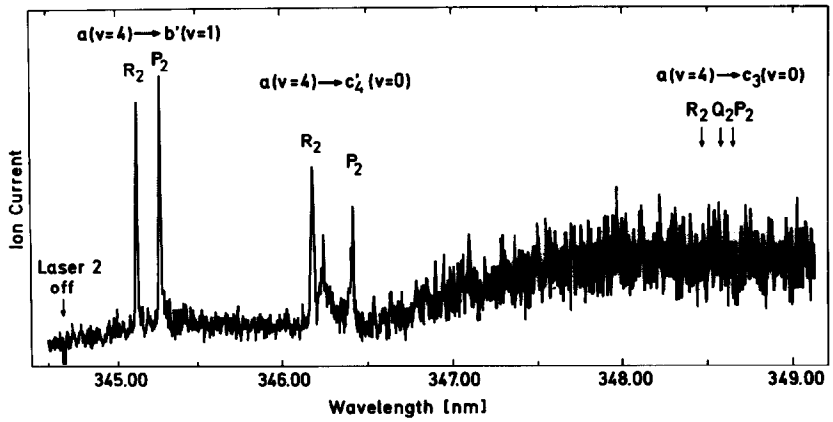

Fig. 8. Scan of the same spectral region as in fig. 7 with 4.5 mJ pulse energy from laser 2 and 1.8 mJ from laser 1; a broad continuum is seen in addition to the resonances which is indicative of a repulsive third intermediate state above the ionization threshold. The noise of the continuum corresponds to the shot-to-shot fluctuations of the two-laser REMPI signal (no signal averaging applied).

energy, with not extremely critical adjustment of the beam overlap.

One way to explain the absence of signal is to assume fast photodissociation of the neutral molecule in the region around 7500 cm^{-1} above the ionization threshold corresponding to about 347 nm from laser 2. Some indication of this resulted from repeating the zero-delay experiment with higher pulse energy (4.5 mJ from laser 2, and 1.8 mJ UV from laser 1). A broad continuum became apparent (see fig. 8) in addition to the resonances. It grew with the wavelength of laser 2. This increase is stronger than shown in the figure because the signal is not divided by the pulse energy of laser 2 which decreases rapidly above 347 nm. The continuum is observed only for high intensities which suggests absorption of more than one additional photon from laser 2. Laser 1 was also found to have a distinct influence on the magnitude of the continuum signal which is reasonable because this laser is focused tighter than laser 2 because of the chromatic aberration of the lens. The threshold condition was approximately 2 mJ for laser 2 and 1 mJ for laser 1. Though a full explanation of these observations is not possible we tend to conclude that the continuum is due to multi-photon ionization out of the a $^1\Pi_g$ state resonantly enhanced by a repulsive state. If this repulsive state were located at about 7500 cm^{-1} above the ionization threshold, which is the excess energy for ionization with laser 2, this would explain the lack of two-colour ion signal for the 30 ns delay.

We tested a third two-colour scheme to prepare $v_+=0$ ions. As indicated at the beginning of this section the photoelectron spectra for 3+1 photon ionization via $c_3(v=0)$ reveal that the A $^2\Pi_u$ ion signal amounts to merely 25% of the X $^2\Sigma_g^+$ ($v_+=0$) signal in this case [38].

This moderate A state population can be eliminated by fluorescence decay without producing too much vibrationally excited N_2^+ (X). The lifetime of the A state is 10 μs [36]. Therefore, for sufficiently long ion flight times (>40 μs) almost all the A state ions decay to the ground state before the beam reaches the collision zone. As one concludes from the Franck–Condon factors [36] and the relative A($v_+=0$, 1) photoelectron signals, 43% of the A state ions decay to X($v_+=0$) and less than 24% to any single X($v_+>0$) level. Thus, any contribution in an X($v_+>0$) level due to fluorescence decay will be less than 5% of the $v_+=0$ population.

The excess energy of the $N_2^+ \leftarrow c_3(v=0) \leftarrow a \leftarrow N_2(X)$ excitation scheme does not perfectly coincide with that of Pratt et al. (13184 cm^{-1}). But the discrepancy is not more than several hundred wavenumbers if one selects a $^1\Pi_g(v'=0$ or 1) as the first intermediate level. We preferred a($v'=1$) because of the much higher Franck–Condon factor [36]. Laser

2 is run with rhodamine 6G dye and frequency doubled. Because this wavelength nearly equals the second harmonic wavelength of laser 1 we could not combine both beams with a dichroic mirror as in the other experiments. The UV beam for laser 2 was therefore directed into the ion source anti-parallel to the other UV beam. An $f=50$ cm lens was used to narrow the beam, placed about 46 cm away from the focus of laser 1. This yields a wider beam than in the earlier experiment which allows us to maintain good beam overlap for a long period. In contrast to the $a(v'=4)$ experiment the polarizations of the two lasers were mutually perpendicular at the ion source. A measurement of the polarization dependence of the two-colour REMPI signal as in the case of the $a(v'=4)$ experiment was not possible.

Scans of laser 2 across the region of the $c_3 \leftarrow a$ (0, 1) and $c'_4 \leftarrow a$ (0, 1) bands with laser 1 tuned to the S_0 line of the $a \leftarrow X$ (1, 0) band are shown in fig. 9. The conditions were 2.2 mJ UV from laser 1, 0.25 mJ from laser 2 for the upper trace and less for the higher-resolution lower trace. No delay was applied between both lasers. Several differences are found with respect to fig. 7. The ionization out of $c_3(v=0)$ is stronger for the new wavelength of laser 2. The Q_2 line of the $c_3 \leftarrow a$ band is present, unlike as in fig. 7, and is saturated as well as the P_2 and R_2 lines (the saturation thresholds were between 1.5 and 3 μJ, depending on the Hönl–London factors; this is slightly higher than for the $a(v'=4)$ case discussed above because of the softer focusing). On the other hand, the $b' \leftarrow a$ (1, 1) resonances do not appear at all. The last difference is the much stronger 2+2 photon background. This is most likely due to the fact that the three-photon energy for laser 1 is rather close to the $b'(v=3)$ and $o_3(v=0)$ levels. The influence of states near the three-photon energy for a $^1\Pi_g(1 \leqslant v' \leqslant 4)$ and a resulting non-Franck–Condon behaviour of the 2+2 photon signal will be discussed in a separate publication [40].

By enhancement of the UV pulse energy of laser 1 to more than 3 mJ, the $c_3 \leftarrow a$ triplet and the $c'_4 \leftarrow a$ doublet become equal in size. More than 5×10^4 ions per pulse were collected by the ion detector. At the same time, the 2+2 photon background begins to exceed the resonant signal. However, a comparison of the dependences of the resonant and non-resonant

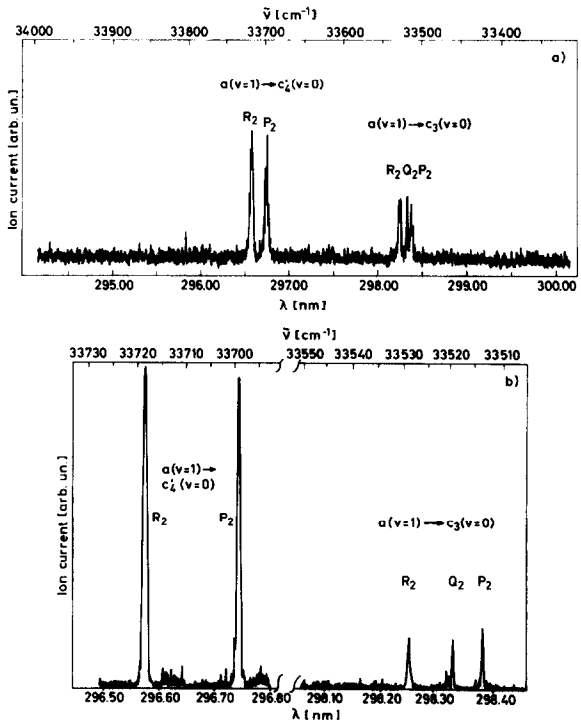

Fig. 9. Scans of laser 2 across the transition from the a $^1\Pi_g(v'=1, J'=2)$ level to the $c'_4(v=0)$ and $c_3(v=0)$ Rydberg states (see text). Upper trace (a): the lines were recorded with enhanced intensity of laser 2 for better visibility (laser 1: 2.2 mJ UV, laser 2: 0.25 mJ UV). Lower trace (b): Partial scans of the two bands with moderate intensity of laser 2 for improved resolution (laser 1: 1.2 mJ, note the reduced 2+2 photon background with respect to the upper trace).

signals on the UV pulse energy from laser 1 reveals that, if laser 2 hits a resonance, the 2+2 channel is entirely depleted, as one would expect.

A suppression of the 2+2 photon background by still softer focusing is not reasonable under our present conditions. The use of, e.g., an $f=50$ cm lens would not reduce the population in the $a(v'=1)$ state by much, but the ionizing step would be pumped less efficiently due to the limited maximum pulse energy of laser 1.

3.6. Selection of N_2^+ in $X(v_+=1)$

As a first step towards the preparation of nitrogen ions in the $X(v_+=1)$ level the following excitation pathway was tested:

$N_2^+ \leftarrow c_3(v=1)$

or

$c_4'(v=1) \leftarrow a(v'=7) \leftarrow N_2(X)$.

The choice of $a(v'=7)$ as the first intermediate level limits the excess energy to 7400 cm^{-1} for ionization with laser 2, i.e., well below the $A\,^2\Pi_u$ state threshold. Because of the predissociation of the $a\,^1\Pi_g$ state for levels with $v \geqslant 7$ temporal separation of the two lasers is not possible. Consequently, the ionization of the Rydberg molecules with laser 1 can be supposed to be at least as relevant as that with laser 2. The excess energy for this process ($\geqslant 20500$ cm^{-1}) is lower than the $B\,^2\Sigma_u^+$ state threshold, but allows many vibrational levels of the A state to be populated.

Preliminary scans of laser 2 across the $c_3 \leftarrow a$ (1, 7) and $c_4' \leftarrow a$ (1, 7) bands, with laser 1 set to the $a \leftarrow X$ (7, 0) S_0 line, are depicted in fig. 10. The pulse energy of laser 2 (2.0 mJ) is ten times higher than the UV pulse energy of laser 1 (0.2 mJ) in order to favour the ionization with laser 2. Both lasers are focused with the same lens ($f=20$ cm). Almost 10^4 ions are detected by the channel plate. The high intensity results in substantial line broadening. The asymmetry of the lines indicates an ac Stark effect or interaction with a continuum. The line strengths of the P_2, Q_2 and R_2 are not constant in contrast to our expectations for saturated transitions.

This excitation scheme obviously has to undergo a detailed vibrational state analysis. For this purpose, a photoelectron spectrometer is currently being set up. In particular, the influence of the high intensity of laser 2 on the ionic state distribution has to be examined. However, laser 2 might also fail to ionize the Rydberg molecules as it was the case for the $v_+=0$ excitation scheme via $a(v'=4)$. The excess energy is nearly the same as in the earlier experiment so that we cannot exclude that one causes photodissociation rather than photoionization.

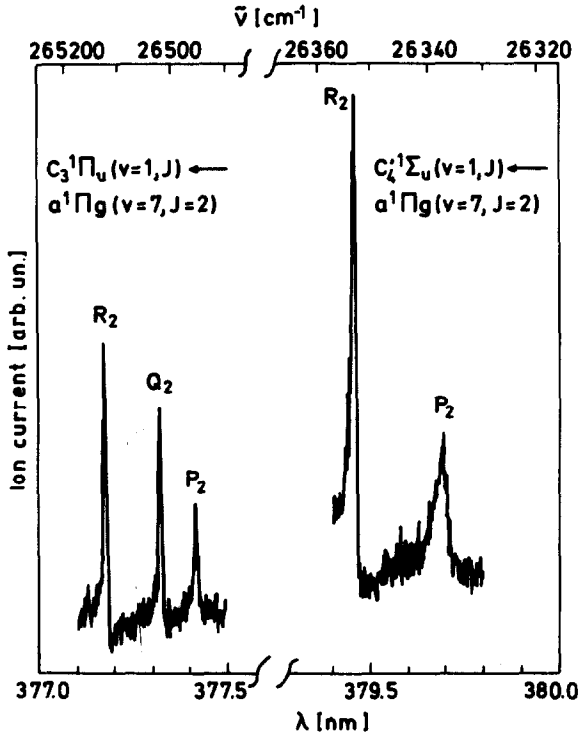

Fig. 10. Scans of laser 2 across the transitions from the $a\,^1\Pi_g(v'=7, J'=2)$ level to the c_3 and c_4' ($v_+=1$) Rydberg levels (see text).

4. Discussion

In the experiments described in section 3 we have tested several efficient REMPI schemes for the generation of vibrationally cold N_2^+ ions in the $X\,^2\Sigma_g^+$ state. Single-laser 2+1 REMPI via $a(v'=10)$ and two-laser 2+1+1 REMPI via $a(v'=1)$ and $c_3(v=0)$ were shown to be the most promising excitation schemes for an intense pulsed source of cold ions. A first experiment was made to prepare N_2^+ in the $v_+=1$ level. The necessary conditions for optimum results were characterized.

4.1. Single-laser experiments

The existence of $X\,^2\Sigma_g^+$ ($v_+=0$) ions in the 2+1 REMPI experiment was proved by LIF of the photoions. The fluorescence experiment also allowed us to determine the rotational propensity or selection rules for this ionization scheme. For S branch excitation in the $a \leftarrow X$ transition the ionization was found to proceed with no change of rotational angular momentum.

LIF of photoions is rather difficult to achieve because of the severe detection losses, as pointed out in section 1. Not too many examples for such studies

have been published (see e.g. refs. [35,51–55]). Refs. [51–53] report on LIF of jet-cooled photoions and refs. [35,54,55] on measurements in a static cell. These experiments could benefit from enhanced ion densities (and also sometimes high ionization rates) which were not accessible under our conditions. Our LIF measurements were carried out at the beginning of the collision-free zone of the molecular beam.

The number of ionic rotational levels which can be populated by photoionization out of a single rotational level is usually quite limited. This is explained by angular momentum conservation plus the restricted number of partial waves for the outgoing electron due to centrifugal barriers [28]. Dixit and McKoy [24] derived selection rules for $n+1$ photon ionization. If the resonant intermediate state as well as the ionic state are characterized by Hund's case (b) the following rule applies:

$$N_+ - N_i + l + p_+ + p_i = \text{odd}\,, \qquad (2)$$

where the indices + and i refer to the ionic and intermediate state, respectively, N is the rotational quantum number, $p=0$ for Σ^+ and Π^+ states and $p=1$ for Σ^- and Π^- states, and l is the angular momentum of the outgoing electron.

For our 2+1 REMPI experiment, the ion+electron symmetry has to be "*ungerade*" because the ionizing transition is a single-photon transition. The ionic ground state being "*gerade*" implies odd values for l. For S branch excitation of the a $^1\Pi_g(v'=10)$ level we populate the Π^+ component of this state. Hence, eq. (2) yields $\Delta N = N_+ - N_i = \text{even}$, in agreement with our observation of a $\Delta N=0$ propensity rule. For P or R branch excitation one would expect $\Delta N=\text{odd}$ because $p_i=1$. However, the P and R lines in the two-photon spectra were too weak to allow successful LIF detection for these two branches.

Our observation of a more or less single ionic rotational level for both S branch lines selected in the a←X (10, 0) band (fig. 6) is in clear contrast to the observations of Ebata et al. [54] who, in a static cell experiment with excitation of the a←X (1, 0) band, observed a substantially larger number of ionic rotational levels for 2+2 photon ionization. Their experiments were carried out at elevated pressures. Thus, their observation of population of a multitude of rotational lines and, in particular, of levels with either parity is ascribed to collisional energy transfer. Relaxation phenomena of N_2^+ rotational and vibrational levels were investigated by the same authors in a subsequent paper and were found to be rather fast [35].

Sha et al. [56] in a study of $N_2(a)$–$N_2(X)$ collisions, point out that such a parity change can only occur in a collision of the excited state molecule with ground state molecules of the opposite parity. In fact, Ebata et al. observed the same 2:1 even:odd-level intensity alternations as Sha et al. in their spectrum for 10 Torr N_2 pressure (upper trace of fig. 4 in ref. [54]) which exactly correspond to the degeneracies of the even and odd rotational levels in the X $^1\Sigma_g^+$ state. This suggests that the explanation by Sha et al. also applies to the case of $N_2^+(X)$–$N_2(X)$ collisions. The intensity alternation is much less pronounced in the LIF spectrum for 1 Torr (lower trace of fig. 4 in ref. [54]), possibly due to a worse signal-to-noise ratio. Again, both parities occur. Thus, in agreement with the conclusion of Ebata et al. from their observation of so many populated rotational levels, we are convinced that the nascent rotational distribution cannot be derived from the results of ref. [54].

In our case, where molecular beam conditions prevail, and also in view of the short detection interval, we can clearly rule out rotational relaxation. Fujii et al. [35] report the onset of rotational redistribution for a N_2 pressure as high as 1 Torr and 35 ns delay between the ionizing and the LIF laser. Our observation of minor contributions in the LIF spectrum from the neighbouring levels to those levels which satisfy the $\Delta N=0$ selection rule cannot be ascribed to collisional effects.

The peaks in the LIF spectra which correspond to ionization with $\Delta N=\pm 1$ might, in principle, be ascribed to the excitation of autoionizing Rydberg states. The symmetry selection rules for autoionization, again, predict the population of either even or odd rotational levels of the ion [57]. However, since autoionization is just a perturbation [57] we expect the validity of eq. (2) also in this case and consequently $\Delta N=0$. In addition, careful inspection of the single-photon ionization spectra of Dehmer et al. [58] shows that there is no autoionizing level at our final energy (the frequencies of many of the lines can be found in ref. [59]).

The most probable explanation is that the intensity of laser 1 was slightly too high for a pure 2+1 photon

process. 2+2 photon absorption may cause ionization with ΔN=odd, which, as discussed above, is not clarified by the results of ref. [54]. The magnitude of the satellite lines in fig. 6, however, suggests that the 2+2 photon effect should be suppressed by choosing an $f \geq 35$ cm lens as in the case of the two-colour experiments (sections 3.2 and 3.5).

The lowest rotational level which can be prepared by the efficient S branch excitation in the 2+1 REMPI process is therefore $N_+ = 2$. If one tunes laser 1 to the much weaker R_0 and P_2 lines $N_+ = 0$ might also become accessible because eq. (2) yields ΔN=odd for these cases. But we see no reason why $\Delta N = -1$, which yields $N_+ = 0$, should have a higher probability than $\Delta N = +1$. Thus, preparation of N_2^+ exclusively in the absolute ground state ($v_+ = N_+ = 0$) with this method is rather unlikely.

4.2. Two-laser experiments

The calculation of the accessible ionic rotational levels with eq. (2) is different in the case of the two-colour experiments. Since the final intermediate state (c_3 or c_4') has "*ungerade*" symmetry, only even values of l are possible. For the c_4' state this yields ΔN=odd for S branch excitation of the a←X transition. For the c_3 state, the c_3←a P and R branches excite the Π^+ component of this state, hence ΔN=odd. For the Q branch, which excites the Π^- component, we get ΔN=even. S branch excitation of the a←X transition is assumed throughout.

All these selection rules were verified in a very recent LIF study by Fujii et al. [35]. For ionization via $c_4'(v=0)$ ionic rotational levels with $\Delta N = \pm 1, \pm 3$ were found to be populated, for ionization via $c_3(v=0)\Pi^+$, $\Delta N = 0, \pm 2$, and for $c_3(v=0)\Pi^-$, $\Delta N = \pm 1, \pm 3$. Because of these careful measurements we did not continue our own LIF experiments in progress.

Again, as in the case of 2+1 REMPI, ionization exclusively in the ($v_+ = 0, N_+ = 0$) level seems not to be conceivable with such an excitation scheme. Only reduction of the excess energy to below the $N_+ = 2$ ionization threshold may suppress internal excitation of the ion. This is not possible with just two tunable lasers for our excitation scheme involving the $a\,^1\Pi_g$ and c_3, c_4' states.

We found that ionization via $c_3(v=0)$ is more than twice as efficient for $a(v'=1)$ and for $a(v'=4)$ as the first intermediate level. This may be explained by a higher ionization cross section at the lower excess energy, by eventual fragmentation losses in the final step of the latter excitation pathway, but also by the presence of weak autoionization in the first case. The LIF spectra by Fujii et al. conform to the expectations from eq. (2) for direct ionization into the $X\,^2\Sigma_g^+$ state. But autoionization results in just the same selection rule [57]. Autoionization may also yield a relative A state population of the ion which is higher than that measured by Pratt et al. [38] for an excess energy slightly different from ours. Fluorescence decay of the A state during the flight of the ions towards the collision zone as proposed in section 3.5 would increase the fraction of $X(v_+ > 0)$ ions with respect to those in $X(v_+ = 0)$ over the 5% estimated for the case of missing autoionization. Any final conclusion will have to come from an experiment which detects the autoionization resonances in this range of excess energies (e.g., with a third tunable REMPI laser) or from PES.

The two-colour experiments with excitation of $a(v'=4)$ as the first intermediate level and a delay of 30 ns between the two lasers failed to yield ion signal enhanced by the c_4'←a (0, 4) resonance. We concluded fast fragmentation of the neutral molecules in the region around 7500 cm^{-1} above the ionization threshold, which was supported by the observation of a broad continuum for elevated intensities (see section 3.5). A similar process was recently demonstrated for H_2 by Trickl et al. [60] with single-laser 1+1 XUV+UV REMPI via $B\,^1\Sigma_u^+$. When ionizing via the lower vibrational levels of the B state H^+ formation was observed as a minor channel. The proton contribution was found to become dominant when tuning the XUV frequency to the (14,0) band. This increase of dissociative ionization was tentatively assigned to the presence of a doubly excited repulsive state near the accumulated energy of the XUV and UV photons. The influence of this state on the 3+1 REMPI via $C\,^1\Pi_u$ was discussed by Chupka [61]. Interestingly, the B←X (14,0) R_1 linewidth observed for H_2^+ at 10 mJ of unfocused UV (measured prior to its attenuation by the used monochromator grating [44,62,63]) was more than five times larger than the 2.5 GHz width which was determined at 33 mJ.

The linewidth for H^+ was 2.5 GHz at both pulse energies. The H_2^+/H^+ ratio at 33 mJ was already 3.5. This indicates that the formation of molecular ions requires the absorption of at least two UV photons by $H_2(B)$ which competes with the dissociative channel.

The possible atomic states of nitrogen for such a fragmentation could not be identified. We did not follow the continuum of fig. 8 to its long-wavelength cut-off. If the dissociation limit were, e.g., $N(^2D^\circ)+N(^2P^\circ)$ (excess energy 0.2 eV) as marked in fig. 1 of ref. [36] there might be a chance to prepare ions exclusively in the $X\,^2\Sigma_g^+$ state by reducing the frequency of the ionizing laser to values near the ionization threshold. This was successfully demonstrated by Trickl et al. [44] in a subsequent experiment by using two-colour 1+1 XUV+visible REMPI via $c_4'(v'=0,1)$. Direct XUV excitation of the c_4' state offers the advantage of the unrestricted tunability of the second laser. Unwanted autoionization resonances could be localized in this way [44].

In our two-colour excitation scheme with a $^1\Pi_g$ as the first intermediate state is is therefore worth trying to excite vibrational levels with $v'>4$, in particular the $v'=6$ level which has 13 stable rotational levels [36]. This has become possible with the advent of BBO doubling crystals which we used for the excitation of the $v'=10$ and the $v'=7$ levels. With laser 2 tuned to the $c_4' \leftarrow a$ (0, 6) band, ionization with this laser would yield an excess energy of 4443.6 cm^{-1} (with laser 1 set to the S_0 line) [40,44]. This value is substantially lower than the 7500 cm^{-1} for the $v'=4$ experiment in which we were unable to detect two-colour ion signal when delaying laser 2 with respect to laser 1. Thus, one might be able to overcome the problems of the latter experiment.

After the submission of this paper we were informed about a very recent 2+1+1 REMPI study of nitrogen by Li et al. [64] which involved $a(v'=1)$ and $c_4'(v=0)$, $c_3(v=2)$. These authors noticed that, when laser 2 was delayed with respect to laser 1 by 13 ns, a pronounced dip appeared at the centre of the power-broadened lines ($E \leqslant 100$ μJ). They explained this dip by the fast decay of these short-lived Rydberg states before the intensity of laser 2 is high enough for substantial photoionization.

Such an effect could, in principle, also explain the lack of two-colour ion signal in our experiments with the 30 ns delay, as long as one assumes that the wavelength of the second laser was always set exactly to the dip position. However, there are several arguments which suggest that the depletion of the c_4' state by spontaneous emission cannot be the main reason for the missing resonant enhancement of the ion signal, in particular:

(1) Many of our experiments were carried out with much higher pulse energies. In a few cases more than fifty times the pulse energy reported by Li et al. was applied, which corresponds to a more than twenty times higher power if one assumes that they used a Nd:YAG-pumped dye laser system which typically delivers 7 ns long pulses. Their focusing conditions must have been similar to ours as we conclude from the magnitude of the power broadening.

(2) We found that ionization out of $c_4'(v=0)$ is particularly efficient (see section 2.5).

(3) We never saw any dip for a 15 ns delay. A few spectra were taken with a 22 ns delay which reduces the time overlap of the two laser pulses to just one or two nanoseconds. In this case, a 80% dip was observed for 30 μJ pulse energy ($f=20$ cm). For 70 μJ, the depth of the dip was already reduced to about one third of the peak height of the $c_4' \leftarrow a$ (0, 4) lines. A pulse energy of 5 mJ, given a measured risetime of 4 ns, delivers the corresponding intensity after 50 ps already. This is much shorter than the reported 0.9 ns lifetime of the $c_4(v=0)$ level [65]. In any case, a two-colour ion signal should have been observable for the 30 ns delay.

Another puzzle is the very size of the Q_2 line for ionization via $c_3(v=0)$ with both laser beams entering the chamber from the same side. This effect was observed by us for excitation via $a(v'=4)$ in the first step and confirmed for $a(v'=1)$ by Ebata et al. [54]. For anti-parallel laser beams we found, in contrast to this, complete saturation of the Q_2 line for the $a(v'=1)$ pathway for a pulse energy from laser 2 as low as 3 μJ, which is the saturation threshold (see section 3.5).

Ebata et al. explain the higher intensity of the P and R lines by "intensity borrowing" from the stronger $c_4'\,^1\Sigma_u^+ \leftarrow a\,^1\Pi_g$ transition. This transition is excited from the Π^+ component of the $a\,^1\Pi_g$ state and, thus, exhibits only P and R lines (see figs. 7 and 9). According to Ebata et al., strong mixing of the c_3 and the c_4' state leads to enhancement of the P_2 and R_2

line strengths in the $c_3 \leftarrow a$ transition, whereas the Q_2 line remains weak since it is absent in the $c'_4 \leftarrow a$ transition.

Our findings at least question this interpretation. For anti-parallel laser beams we find that the saturation threshold pulse energy for the Q_2 line is roughly the same as that for the P_2 and R_2 line. For the parallel configuration of the beams the Q_2 line becomes just about half as intense as the P_2 and the R_2 line for pulse energies which are 50 to 100 times higher than the energy for the onset of saturation. This factor is perhaps too high to justify an interpretation by "intensity borrowing" from the $c'_4 \leftarrow a$ transition. It would imply that the $c_3 \leftarrow a$ (0, 4) band without mixing, as represented by the Q branch, is more than 1500 times weaker than the $c'_4 \leftarrow a$ (0, 4) band, which results from multiplying the above factor by the ratio of the saturation thresholds for the P_2 and R_2 lines for both bands (see section 3.5).

We assume that these numbers are similar for $a(v'=1)$ as the first intermediate level which case was studied by Ebata et al. [54] with both lasers parallel. Though we used an anti-parallel configuration for this excitation pathway a qualitative comparison with ref. [54] is possible. From the relative line intensities of the different bands in ref. [54] and in our experiment we can conclude that the intensity from laser 1 is roughly the same in both experiments. Unfortunately, Ebata et al. do not specify their focusing conditions. However, the UV pulse energy from their Nd:YAG-pumped dye laser system of up to 10 mJ suggests a focal length up to 1 m. Even for such a long focal length one may assume complete saturation of the transition from the $a\,^1\Pi_g$ state to the Rydberg states with the pulse energy of 0.3 mJ for laser 2 reported by Ebata et al. This would deteriorate the 1:10 ratio of the Q_2 line strength with respect to the P_2 and the R_2 line strengths which was given by these authors, in better agreement with ours results.

A full solution to this interesting problem would require further, more detailed investigations which were beyond the scope of the present paper. Such experiments should also include a repetition of the polarization studies which were not complete in this study (see section 3.5).

5. Conclusion

We have demonstrated that single-laser 2+1 REMPI via $a\,^1\Pi_g(v'=10)$ is a suitable method to produce a large quantity ($\geqslant 10^5$) of vibrationally cold N_2^+ ions with little rotational excitation. Preparation of vibrationally selected N_2^+ in the $X\,^2\Sigma_g^+$ state by two-colour REMPI via the c_3 and c'_4 Rydberg states was found to have certain limitations in contrast to the very favourable situation for the vibrational state selection in the $A\,^2\Sigma_u^+$ state reported by Pratt et al. for 3+1 REMPI via $o_3\,^1\Pi_u(v'=0, 1)$ [20]. These limitations, which are outlined in the preceding sections, originate from generation of ions not only in the X, but also in the A state, which is a result of the strong mixing of the Rydberg states of N_2 with states for which A state ionization is possible in a single-electron transition [38]. Thus, in nearly all cases, the excess energy of the ionizing step has to be kept below the A state ionization threshold, which is done by selecting a sufficiently low frequency for laser 2. One exception is ionization via $a(v'=1)$ and $c_3(v=0)$ where the $A\,^2\Sigma_u^+$ contributions are much smaller than those in $X\,^2\Sigma_g^+$ and can be substantially reduced by fluorescence decay without producing too much vibrationally excited N_2^+ in the X state. In the other cases a $^1\Pi_g$ state vibrational levels with $v' \geqslant 4$ ($v' \geqslant 7$ for preparation of the $v_+ = 1$ level) have to be excited in the first step. The problems mentioned above arise from the necessary temporal separation of the two laser pulses which limits the range of useful a state levels to $v' \leqslant 6$ because of the predissociation of the higher levels. This dramatically reduces the range of possible intermediate levels. Some further reduction may be imposed by fast fragmentation which would limit the useful a state levels for $v_+ = 0$ generation to $v' > 4$. One experiment is under way to test the two-colour ionization via $v' = 6$, which has 13 state rotational levels [36] thus allowing to delay laser 2 with respect to laser 1.

The full potential of the more sophisticated two-colour excitation would only be used if one succeeded in generating a clean $v_+ = 1$ ion beam (or even $v_+ > 1$). PES will be necessary to control the ionic state distribution, particularly in those cases where one works with high excess energies in the ionizing step. Low excess energies, however, can be obtained with a different approach. With higher UV pulse

energies than available from our present dye laser configuration, pumped by a single excimer laser, direct XUV excitation of the Rydberg states from the ground state becomes possible. In this case, the second laser can be tuned to just above the v_+ ionization threshold of interest. This method is quite flexible and should be applicable to a much greater variety of molecules than REMPI with visible and UV light, for which the search for suitable excitation schemes and operating conditions might be quite lengthy as demonstrated in this experiment.

Acknowledgement

We would like to thank Professor T. Keiderling and Dr. E.S. McGinley for their collaboration in different phases of the project. We are particularly indebted to Professor Sha Guohe whose complimentary studies in our laboratory involving the a←X transition of N_2, as well as some of the Rydberg states, were helpful for this project. Dr. H Liebl made valuable suggestions for the design of the mass separator and the ion optics. We thank H. Bauer and R. Maier for their technical assistance. Finally, we thank our reviewer for bringing ref. [64] to our attention.

References

[1] T. Baer, in: Gas Phase Ion Chemistry, Vol. 1, ed. M. Bowers (Academic Press, New York, 1979) ch. 5.
[2] K. Tanaka and I. Koyano, J. Chem. Phys. 69 (1978) 3422.
[3] I. Koyano and K. Tanaka, J. Chem. Phys. 72 (1980) 4858.
[4] T.R. Govers, P.M. Guyon, T. Baer, K. Cole, H. Fröhlich and M. Lavollée, Chem. Phys. 87 (1984) 373.
[5] M.A. Johnson, M.L. Alexander, I. Hertel and W.C. Lineberger, Chem. Phys. Letters 105 (1984) 374.
[6] W.A. Chupka and J. Berkowitz, J. Chem. Phys. 51 (1969) 4244.
[7] P.M. Dehmer and W.A. Chupka, J. Chem. Phys. 65 (1976) 2243.
[8] S.L. Anderson, F.A. Houle, D. Gerlich and Y.T. Lee, J. Chem. Phys. 75 (1981) 2153.
[9] F.A. Houle, S.L. Anderson, D. Gerlich, T. Turner and Y.T. Lee, Chem. Phys. Letters 82 (1981) 392.
[10] S.L. Anderson, T. Turner, B.H. Mahan and Y.T. Lee, J. Chem. Phys. 77 (1982) 1842.
[11] T. Turner, O. Dutuit and Y.T. Lee, J. Chem. Phys. 81 (1984) 3475.
[12] J.D. Shao and C.Y. Ng, J. Chem. Phys. 84 (1986) 4317.
[13] J.T. Meek, S.R. Long and J.P. Reilly, J. Phys. Chem. 86 (1982) 2809.
[14] S.R. Long, J.T. Meek and J.P. Reilly, J. Chem. Phys. 79 (1983) 3206.
[15] J.C. Miller and R.N. Compton, Chem. Phys. Letters 93 (1982) 453.
[16] S.L. Anderson, G.T. Kubiak and R.N. Zare, Chem. Phys. Letters 105 (1984) 22.
[17] S.T. Pratt, P.M. Dehmer and J.L. Dehmer, Chem. Phys. Letters 105 (1984) 28.
[18] S.T. Pratt, P.M. Dehmer and J.L. Dehmer, J. Chem. Phys. 85 (1986) 3379.
[19] M.O. O'Halloran, S.T. Pratt, P.M. Dehmer and J.L. Dehmer, J. Chem. Phys. 87 (1987) 3288.
[20] S.T. Pratt, P.M. Dehmer and J.L. Dehmer, J. Chem. Phys. 80 (1984) 1706.
[21] W.E. Conaway, R.J.S. Morrison and R.N. Zare, Chem. Phys. Letters 113 (1985) 429.
[22] R.J.S. Morrison, W.E. Conaway and R.N. Zare, Chem. Phys. Letters 113 (1985) 435;
R.J.S. Morrison, W.E. Conaway, T. Ebata and R.N. Zare, J. Chem. Phys. 84 (1986) 5527.
[23] W.E. Conaway, T. Ebata and R.N. Zare, J. Chem. Phys. 87 (1987) 3447.
[24] S.N. Dixit and V. McKoy, Chem. Phys. Letters 128 (1986) 49.
[25] L. Åsbrink, Chem. Phys. Letters 7 (1970) 549.
[26] Y. Morioka, S. Hara and M. Nakamura, Phys. Rev. A 22 (1980) 177.
[27] J.E. Pollard, D.J. Trevor, J.E. Reutt, Y.T. Lee and D.A. Shirley, J. Chem. Phys. 77 (1982) 34.
[28] S.T. Pratt, P.M. Dehmer and J.L. Dehmer, J. Chem. Phys. 78 (1983) 4315.
[29] W.G. Wilson, K.S. Viswanathan, E. Sekreta and J.P. Reilly, J. Phys. Chem. 88 (1984) 672.
[30] K. Müller-Dethlefs, M. Sander and E.W. Schlag, Z. Naturforsch. 39a (1984) 1089.
[31] K. Müller-Dethlefs, M. Sander and E.W. Schlag, Chem. Phys. Letters 112 (1984) 291.
[32] K.S. Viswanathan, E. Sekreta, E.R. Davidson and J.P. Reilly, J. Phys. Chem. 90 (1986) 5078.
[33] M. Sander, L.A. Chewter, K. Müller-Dethlefs and E.W. Schlag, Phys. Rev. A 36 (1987) 4543.
[34] W. Habenicht, R. Baumann, K. Müller-Dethlefs and E.W. Schlag, Ber. Bunsenges. Physik. Chem. 92 (1988) 414.
[35] A. Fujii, T. Ebata and M. Ito, J. Chem. Phys. 88 (1988) 5307.
[36] A. Lofthus and P.H. Krupenie, J. Phys. Chem. Ref. Data 6 (1977) 113, and references therein.
[37] S. Opitz, D. Proch and T. Trickl, State Selective Ionization of Nitrogen by Resonance-Enhanced Photoionization of Cold Jet, paper presented at the Conference on Lasers and Electro-Optics, 9–13 June 1986, San Francisco, USA. Book of Abstracts, p. 72.

[38] S.T. Pratt, P.M. Dehmer and J.L. Dehmer, J. Chem. Phys. 81 (1984) 3444.
[39] H. Schmoranzer, P. Hartmetz, D. Marger and J. Dudda, J. Phys. B 22 (1989) 1761.
[40] D. Proch and T. Trickl, to be published.
[41] D. Proch and T. Trickl, Rev. Sci. Instrum. 60 (1989) 713.
[42] W. Eckstein and H. Verbeek, Max-Planck-Institut für Plasmaphysik, Laborbericht IPP 9/1 (1972).
[43] H. Kogelnick and T. Li, Appl. Opt. 5 (1966) 1550.
[44] T. Trickl, E. Cromwell, Y.T. Lee and A.H. Kung, J. Chem. Phys. 91 (1989) 6006.
[45] R.A. Gottscho, R.W. Field, K.A. Dick and W. Benesch, J. Mol. Spectry. 74 (1979) 435.
[46] R. Herman, Compt. Rend. Acad. Sci. (Paris) 217 (1943) 141.
[47] R. Herman, Ann. Phys. (Paris) 20 (1945) 241.
[48] R.W. Nicholls, Can. J. Phys. 40 (1962) 523.
[49] W. Benesch, D. Rivers and J. Moore, J. Opt. Soc. Am. 70 (1980) 792.
[50] W.J. Marinelli, W.J. Kessler, B.D. Green and W.A.M. Blumberg, J. Chem. Phys. 91 (1989) 701.
[51] M. Heaven, T.A. Miller and V.E. Bondybey, J. Chem. Phys. 76 (1982) 3831.
[52] L.F. Dimauro, M. Heaven and T.A. Miller, Chem. Phys. Letters 104 (1984) 526.
[53] L.F. Dimauro and T.A. Miller, Chem. Phys. Letters 138 (1987) 175.
[54] T. Ebata, A. Fujii and M. Ito, J. Chem. Phys. 91 (1987) 3125.
[55] J. Xie and R.N. Zare, Chem. Phys. Letters 159 (1989) 399.
[56] G. Sha, D. Proch and K.L. Kompa, J. Chem. Phys. 87 (1987) 5251.
[57] G. Herzberg, Molecular Spectra and Molecular Structure, Vol. 1. Spectra of Diatomic Molecules, 2nd Ed. (Van Nostrand, Princeton, 1950).
[58] P.M. Dehmer, P.J. Miller and W.A. Chupka, J. Chem. Phys. 80 (1984) 1030.
[59] M. Ogawa and Y. Tanaka, Can. J. Phys. 40 (1962) 1593.
[60] T. Trickl, E. Cromwell, A.H. Kung and Y.T. Lee, Proceedings of the Symposium on Atomic and Surface Physics (SASP 90), 1990, submitted.
[61] W.A. Chupka, J. Chem. Phys. 87 (1987) 1488.
[62] E. Cromwell, T. Trickl, Y.T. Lee and A.H. Kung, Ultra-Narrow Bandwidth XUV-VUV Laser System, Rev. Sci. Instrum. 60 (1989) 2888.
[63] T. Trickl, M.J.J. Vrakking, E. Cromwell, Y.T. Lee and A.H. Kung, Phys. Rev. A 39 (1989) 2948.
[64] L. Li, W.A. Chupka and S.T. Pratt, J. Chem. Phys. 90 (1989) 606.
[65] J.E. Hesser and K. Dressler, J. Chem. Phys. 45 (1966) 3149.